



Desipramine reverses remote memory deficits by activating calmodulin-CaMKII pathway in a *UTX* knockout mouse model of Kabuki syndrome

Lei Chen,¹ Yuting Li ,¹ Minggang Liu,^{2,3} Zhaohui Lan,¹ Xu Zhang,¹ Xiujuan Yang,¹ Qian Zhao,¹ Shuai Wang ,¹ Longyong Xu,⁴ Ying Zhou,¹ Yifang Kuang,¹ Tatsuo Suzuki,⁵ Katsuhiko Tabuchi,⁵ Eiki Takahashi,¹ Miou Zhou,⁶ Charlie Degui Chen,⁴ Tianle Xu,² Weidong Li^{1,7}

To cite: Chen L, Li Y, Liu M, *et al.* Desipramine reverses remote memory deficits by activating calmodulin-CaMKII pathway in a *UTX* knockout mouse model of Kabuki syndrome. *General Psychiatry* 2024;**37**:e101430. doi:10.1136/gpsych-2023-101430

► Additional supplemental material is published online only. To view, please visit the journal online (<https://doi.org/10.1136/gpsych-2023-101430>).

LC, YL, ML and ZL contributed equally.

Received 26 November 2023
Accepted 12 June 2024



© Author(s) (or their employer(s)) 2024. Re-use permitted under CC BY-NC. No commercial re-use. See rights and permissions. Published by BMJ.

For numbered affiliations see end of article.

Correspondence to

Weidong Li; liwd@sju.edu.cn

ABSTRACT

Background Kabuki syndrome (KS) is a rare developmental disorder characterised by multiple congenital anomalies and intellectual disability. *UTX* (ubiquitously transcribed tetratricopeptide repeat, X chromosome), which encodes a histone demethylase, is one of the two major pathogenic risk genes for KS. Although intellectual disability is a key phenotype of KS, the role of *UTX* in cognitive function remains unclear. Currently, no targeted therapies are available for KS.

Aims This study aimed to investigate how *UTX* regulates cognition, to explore the mechanisms underlying *UTX* dysfunction and to identify potential molecular targets for treatment.

Methods We generated *UTX* conditional knockout mice and found that *UTX* deletion downregulated calmodulin transcription by disrupting H3K27me3 (trimethylated histone H3 at lysine 27) demethylation.

Results *UTX*-knockout mice showed decreased phosphorylation of calcium / calmodulin-dependent protein kinase II, impaired long-term potentiation and deficit in remote contextual fear memory. These effects were reversed by an Food and Drug Administration-approved drug desipramine.

Conclusions Our results reveal an epigenetic mechanism underlying the important role of *UTX* in synaptic plasticity and cognitive function, and suggest that desipramine could be a potential treatment for KS.

INTRODUCTION

Kabuki syndrome (KS) is a rare condition characterised by congenital developmental abnormalities and mental disorders.¹ The underlying causes of KS are still elusive and no effective treatment is available for KS.² *UTX* (ubiquitously transcribed tetratricopeptide repeat, X chromosome), also known as *KMD6A* (lysine demethylase 6A), is a pathogenic risk gene of KS³ and plays an important role in the nervous system.⁴ *UTX* is a pathogenic risk gene of KS that plays an important role in the nervous system. In 2012, Paděřová

WHAT IS ALREADY KNOWN ON THIS TOPIC

- ⇒ Kabuki syndrome (KS) is a rare disorder characterised by congenital anomalies and intellectual disability.
- ⇒ *UTX*, a histone demethylase gene on the X chromosome, is a major risk factor for KS.
- ⇒ Currently, no targeted therapies are available for KS.

WHAT THIS STUDY ADDS

- ⇒ We found that the impairment of long-term potentiation and the deficit in remote contextual fear memory are caused by decreased phosphorylation of calcium / calmodulin-dependent protein kinase II.
- ⇒ These deficits could be rescued by an Food and Drug Administration-approved drug desipramine.

HOW THIS STUDY MIGHT AFFECT RESEARCH, PRACTICE OR POLICY

- ⇒ Our results reveal the mechanism underlying the important role of *UTX* in synaptic plasticity and cognitive function and suggest that desipramine could be a potential treatment for KS.

et al identified heterozygous mutations in the *UTX* gene in 3%–8% of KS cases.⁵ In these cases, researchers found either a total or substantial deletion of the *UTX* gene, with affected individuals exhibiting a wide array of phenotypic features, including typical KS facial features and moderate clinical manifestations.

Histone 3 methylation and demethylation modulate the expression of memory-related genes and are involved in memory consolidation and storage.⁶ *UTX* specifically removes methyl groups from histone 3 that is dimethylated or trimethylated at lysine 27 (H3K27me2/3 methyl group), which promotes gene transcription involved in neural regeneration, development, metabolism and other important physiological

functions in humans and animals.⁷ Previous studies have found that genetic defect in *UTX* affects the development process of neural stem cells and neural crest cells.⁸ However, research on the mechanisms through which *UTX* affects cognition remains lacking.

Long-term potentiation (LTP), particularly in the hippocampus, is recognised as an underlying phenomenon of neural synaptic plasticity and an important mechanism of learning and memory. Therefore, this study aimed to investigate *UTX* functions in synaptic plasticity and performance in contextual fear conditioning with *UTX* conditional knockout (cKO) mice. Additionally, we sought to elucidate the effects of desipramine, a psychotropic medication known to ameliorate cognitive deficits in *UTX* cKO mice.⁹ We hypothesised that the epigenetic mechanism of the *UTX* regulation of the calmodulin-CaMKII pathway is essential for the expression of remote memory.

METHODS AND MATERIALS

Animal husbandry

Male *UTX* hemizygous mice aged 8–12 weeks were used in the study, and the wild-type (WT) littermates were used as the control group for all experiments. Mice were weaned at the fourth postnatal week and maintained on a 12/12-hour light/dark cycle with access to food and water ad libitum.

Contextual fear conditioning

During the training stage, mice were placed in the fear conditioning chamber (Med Associates) of the training context. After exploring the chamber for 2 min, mice received three 0.72 mA foot shocks (2 s each, 1 min interval between the shocks). The training sessions lasted for 5 min. Tests were performed 24 hours and 4 weeks after training. During the test, the mice were placed back into the chamber for 5 min. The behaviour in mice was recorded and analysed using automated motion detection software Actimetrics (Freezeframe4, ACT-712).

Hippocampal slices preparation

After anaesthesia induction, mice aged 8–10 weeks were transcardially perfused with ice-cold oxygenated (95% O₂, 5% CO₂) fresh artificial cerebral-spinal fluid (aCSF). After decapitation, hippocampal slices (300 μm thick) were prepared with a vibrating tissue slicer (Leika, VT1000S, Germany) in cold aCSF. The slices were recovered in a submerged chamber for 30 min at 32°C and then transferred to room temperature in carbogen-bubbled aCSF, for at least 1 hour.

Multielectrode array recordings in hippocampal slices

The procedures were used to prepare the MED64 probe and multichannel field potential recordings. The field excitatory postsynaptic potentials (fEPSPs) evoked in the CA1 area were amplified by a 64-channel amplifier. The test stimulation intensity was adjusted so that an

average of 30%–60% of the maximal synaptic response, according to the input-output curves, was induced. For LTP induction, a 1× high-frequency stimulation (HFS) (100 Hz, 1 s) protocol was used with the same stimulation intensity as the baseline.¹⁰ For quantification of LTP data, the initial slope of fEPSP was measured, normalised and expressed as a percentage change from the baseline level. The number of activated channels (ie, with the fEPSP amplitude higher than -20 μV) and LTP-showing (fEPSP slope increased by at least 20% of baseline) channels were counted.¹¹

Extracellular fEPSP recordings

Recordings were made in a standard submerged chamber with aCSF perfusion at a speed of 2 mL/min at 25°C. Schaffer collaterals were stimulated by a platinum bipolar electrode for a duration of 0.1 ms every 60 s. Data were acquired through Multiclamp 700B and pClamp V.10 software (Molecular Devices). Paired-pulse ratio (PPR) was examined at interstimulus intervals of 50 ms with a stimulation strength that corresponded to 50% of the maximal fEPSP.

Whole-cell recordings of spontaneous excitatory postsynaptic currents (sEPSCs)

CA1 pyramidal neurons were identified under an infrared differential interference contrast microscope in the submerged recording chamber (DAGE-MTI IR1000). Neurons were recorded for 5 min at a holding voltage of -60 mV with 10 μM bicuculline in aCSF perfused at a flow rate of 2 mL/min. sEPSCs were detected by the MiniAnalysis program (Synaptosoft, Decatur, Georgia, USA).

Real-time quantitative PCR

The primers used are shown in online supplemental table 1. Total RNA was isolated following the TRIZOL method protocols. In reverse-transcription quantitative PCR, RNA was reverse-transcribed into cDNA with the kit (Takara RR037A). Real-time quantitative PCR was carried out with SYBR Green PCR Master Mix (Roche 4887352001). The relative expression values for each mRNA were calculated by comparative Ct and were normalised to glyceraldehyde 3-phosphate dehydrogenase.

Transcriptome sequencing

In the transcriptome sequencing experiment, the hippocampus from adult mice (n=3 per group) was dissected and collected as samples for sequencing. RNA library preparation, clustering, sequencing and data analyses were carried out by the Beijing Genomics Institution.

Chromatin immunoprecipitation (ChIP)-quantitative PCR

Samples were prepared from the WT and cKO mice hippocampus with an EZ-ChIP kit (17-371, Merck Millipore). Shear DNA using a sonicator to an optimal DNA fragment size of 200–400 bp. The ChIP-qPCR experiments with samples from the WT and *UTX* cKO groups were carried out using the H3K27me3 antibody (07-449,

Merck Millipore). The primers used are shown in online supplemental table 2.

Western blotting

The protein extracted from the hippocampus was quantified using the DC protein assay (Bio-Rad). Equivalent protein was subjected to 8% or 12% sodium dodecyl sulfate-polyacrylamide gel electrophoresis and transferred electrophoretically to polyvinylidene fluoride membranes. The membranes were incubated with primary antibodies after blocking with 5% skimmed milk (online supplemental table 3). The membranes were then incubated with horseradish peroxidase-conjugated secondary antibody. Blots were visualised using a chemiluminescence approach (ECL system, Merck Millipore) with the Tanon-5200 Chemiluminescent Imaging System (Tanon Science & Technology).

Desipramine treatment

Desipramine (30 mg/kg) was administered to mice in drinking water for 2 weeks before the sample collection or experiments (electrophysiological recording and behavioural test) were performed, and the drug was administered throughout the behavioural test. For the multielectrode array recordings, we perfused desipramine (5 μ M) to acute hippocampal slices for 40 min (from 20 min prior to HFS delivery to 20 min after LTP induction). LTP was induced with HFS (1 train of 100 Hz stimulation for 1 s). For the patch-clamp experiments, desipramine (10 μ M) was applied to slices for 30 min before the 10 min sEPSC recordings.

Analysis of neuronal morphology with rapid labelling

Sagittal brain slices (350–400 μ m thick) were prepared from adult mice and slices were labelled with DiI (Invitrogen, D282). The rapid labelling procedure was performed as previously described.¹² CA1 pyramidal neurons in the hippocampus were examined using an oil-immersion 64 \times objective lens. Images were captured using a TCS SP8 STED 3X multiphoton confocal microscope (Leica) and analysed with Fiji software (ImageJ). The number of branches was counted. The total length of dendrites and intersections was calculated by using Sholl analysis. The average spine density was calculated as the number of spines per dendritic length of 10 μ m. A total of at least 900 μ m of dendrites was analysed for each group.

Brain stereotactic virus injection procedure

Using glass electrodes, a depth of 1.4 mm below the brain surface was targeted for insertion into the CA1 region, with coordinates set at AP=1.9 and ML= \pm 1.5. The injection of virus was carried out at a controlled rate of 50 nL/min, with a total volume of 500 nL administered. The viruses used in this procedure were AAV-Syn-CRE and AAV-CaMKII-CRE.

Statistical analysis

Numerical variables were represented as the mean (standard error of the mean (SEM)) and analysed using

GraphPad Prism software (V.8.3.1). Unpaired two-tailed t-tests were used to evaluate the significant differences between the two groups. The electrophysiology data were analysed using OriginPro 2015 (OriginLab Corporation, USA), clampfit (V.11.0.3), and t-tests or analysis of variance (ANOVA). P values <0.05 were considered statistically significant (* p <0.05, ** p <0.01, *** p <0.001).

RESULTS

UTX cKO mice exhibit remote memory impairments

The targeting vector, with exons 11, 12, 13 and 14 encoding the JmjC demethylase domain of *UTX*, was flanked by two loxP sites (figure 1A). Hemizygous male *UTX*^{f/y} mice were then produced by crossing female *UTX*^{f/f} with male Nestin-cre mice. Genetic deletion of *UTX* was validated at the protein level in the hippocampus and prefrontal cortex by western blotting (figure 1B). *UTX* cKO mice have shorter stature and lower body weight, similar to those observed in individuals with KS (figure 1C,D). In addition, cKO mice exhibited a significant decrease in the dendritic arborisation complexity, total dendritic length and number of branches (online supplemental figure 1). Behavioural tests revealed cognitive deficits in spatial learning and memory in *UTX* cKO mice (online supplemental figure 2). To investigate the effect of *UTX* deletion on cognitive function, *UTX* cKO and WT mice were subjected to a contextual fear conditioning test for learning and memory assessment.¹³ Mice received an aversive stimulus in the conditional chamber and were subsequently tested 24 hours (recent memory) or 4 weeks later (remote memory) for freezing time in that chamber. *UTX* cKO and WT mice displayed no difference in freezing percentage at 24 hours after training (figure 1E). However, the cKO mice showed significantly lower freezing compared with WT mice at 4 weeks after training (figure 1F), indicating that *UTX* gene deletion leads to remote fear memory deficits.

UTX cKO mice show a deficit in synaptic plasticity

We found that HFS-induced LTP was compromised in the *UTX* cKO mice (WT vs *UTX* cKO: 161.0 (5.1)% vs 105.8 (5.7)% of baseline at 120 min after HFS, n =6–7 slices/6–7 mice; figure 1G). Moreover, significantly fewer LTP-showing channels were found in *UTX* cKO hippocampal slices compared with WT hippocampal slices (WT vs *UTX* cKO: 11.7 (2.1) vs 3.7 (1.1); figure 1H). To confirm the role of hippocampal *UTX* in LTP, we recorded LTP in *UTX*^{f/y} mice with the intra-hippocampal injection of AAV-Syn-Cre virus. The data revealed consistent results, showing impaired LTP similar to that observed in cKO mice (online supplemental figure 4). These data demonstrate that *UTX* gene deletion significantly reduces the probability of LTP induction in hippocampal neurons.

Synaptic transmission is the critical cellular basis of memory storage in the brain. To verify whether the basal synaptic transmission was altered in *UTX* cKO mice, we

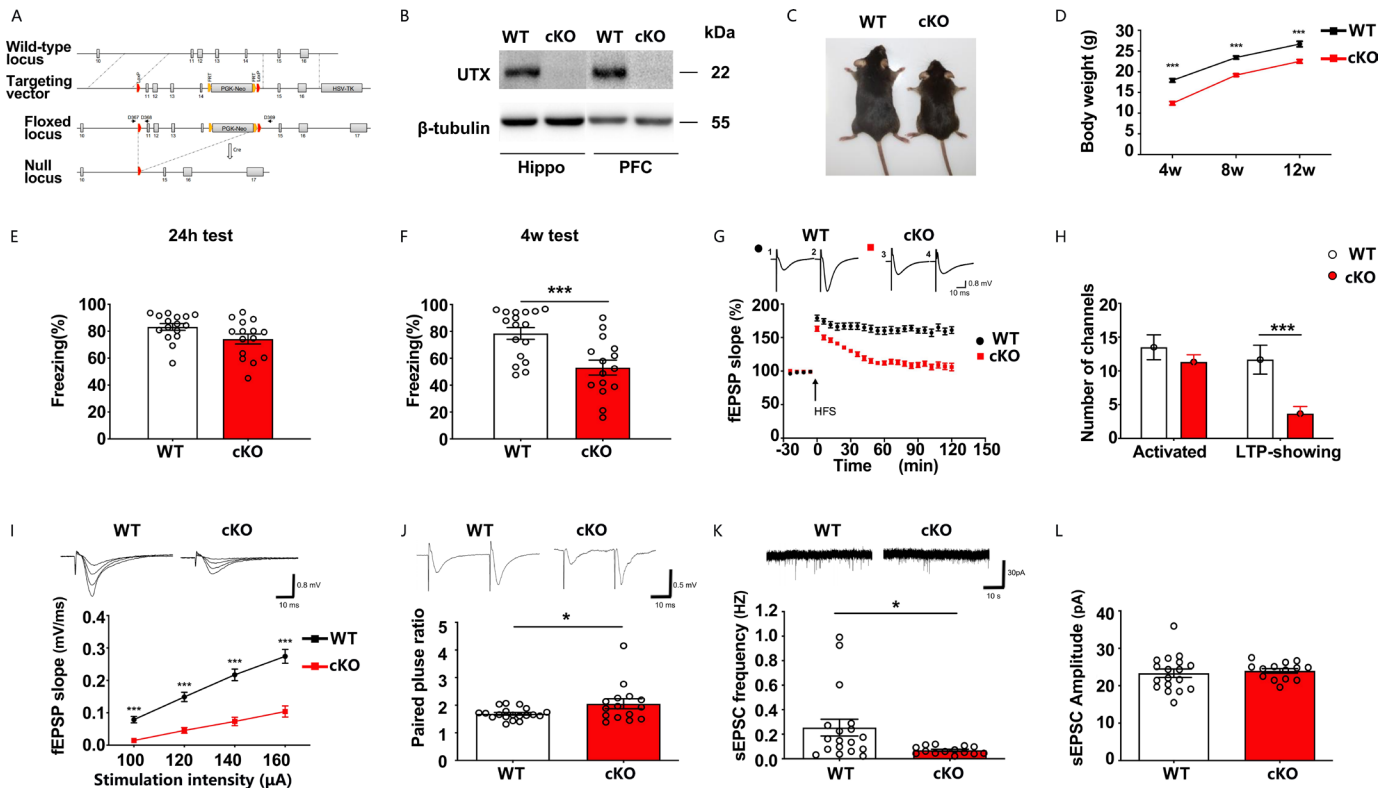


Figure 1 *UTX* cKO mice show impaired cognitive function and LTP and abnormal basal synaptic transmission in hippocampal neurons. (A) Schematic diagram of the construction of the *UTX* cKO mouse model. (B) *UTX* protein levels in the hippocampus and prefrontal cortex of WT and cKO mice were detected by western blotting. (C) From infancy to adulthood, male cKO mice were smaller than WT mice. The image shown depicts male mice at 9 weeks of age. (D) *UTX* cKO mice exhibited decreased body weight compared with WT mice throughout adulthood (WT, $n=17$ at 4, 8 and 12 weeks of age; cKO, $n=12, 14$, and 10 at 4, 8 and 12 weeks of age, respectively; $***p<0.001$, two-way ANOVA). (E, F) Mouse freezing percentage in contextual fear conditioning test at 24 hours and 4 weeks after training (WT, $n=15$; cKO, $n=17$; $***p<0.001$, unpaired t-tests). (G) LTP recordings of fEPSPs induced by a high-frequency stimulation protocol (a train of 100Hz stimulation for 1 s) recorded in hippocampal slices ($n=6$ slices per 6 mice from each group). Representative traces of the averaged baseline responses (left) and the responses during the last 10 min of recordings (right) in WT and cKO mice are shown at the top of the image. (H) The number of activated channels showing fEPSP responses to Schaffer collateral pathway stimulation and LTP-showing channels that responded to the HFS protocol in CA1 neurons from WT and cKO mice ($n=6$ slices per 6 mice from each group, $***p<0.001$, two-way ANOVA). (I) The input-output curve showing the relationship between the slope of fEPSPs and the stimulation intensity at Schaffer collateral-CA1 synapses in hippocampal slices (WT, $n=19$ slices from six mice; cKO, $n=15$ slices from five mice; $***p<0.001$, two-way ANOVA). The representative traces in WT and cKO mice are shown at the top of the image. (J) Paired-pulse ratio measured at intervals of 50 ms (WT, $n=19$ slices from six mice; cKO, $n=15$ slices from five mice; $*p<0.05$, Student's t-test). Representative traces from WT and cKO mice are shown at the top of the image. (K) Quantitative analyses of sEPSC frequency between WT and cKO animals (WT, $n=18$ slices from seven mice; cKO, $n=14$ slices from five mice; $*p<0.05$, Student's t-test). Representative traces of sEPSCs recorded in WT and cKO mice are shown at the top of the image. (L) Quantitative analysis of the sEPSC amplitude between WT and cKO animals (WT, $n=18$ slices from seven mice, cKO, $n=14$ slices from five mice). All data are presented as the mean (SEM). ANOVA, analysis of variance; cKO, conditional knockout; fEPSPs, field excitatory postsynaptic potentials; Hippo, hippocampus; LTP, long-term potentiation; sEPSC, spontaneous excitatory postsynaptic current; PFC, prefrontal cortex; SEM, standard error of the mean; WT, wild type.

analysed the input/output curves of the fEPSPs. The slope of fEPSPs significantly decreased in cKO mice compared with WT mice, indicating a decrease in synaptic strength (figure 1I). Next, to examine short-term plasticity in the cKO mice, the PPR was analysed. Results showed a significantly enhanced PPR in cKO mice compared with WT mice (figure 1J), suggesting that the presynaptic release of neurotransmitters is decreased in the *UTX* cKO mice. Moreover, whole-cell patch clamp recording of the sEPSC showed a significant decrease in sEPSC frequency of CA1 pyramidal neurons in cKO mice (figure 1K) with no

change in sEPSC amplitude (figure 1L), confirming the deficit in presynaptic neurotransmitter release in *UTX* cKO mice.

UTX cKO mice show downregulated calmodulin expression and CaMKII signalling

To explore the molecular mechanism of impaired LTP and memory in *UTX* cKO mice, we conducted transcriptome sequencing and pathway analysis. We identified that calmodulin was associated with the LTP pathway and was downregulated in *UTX*

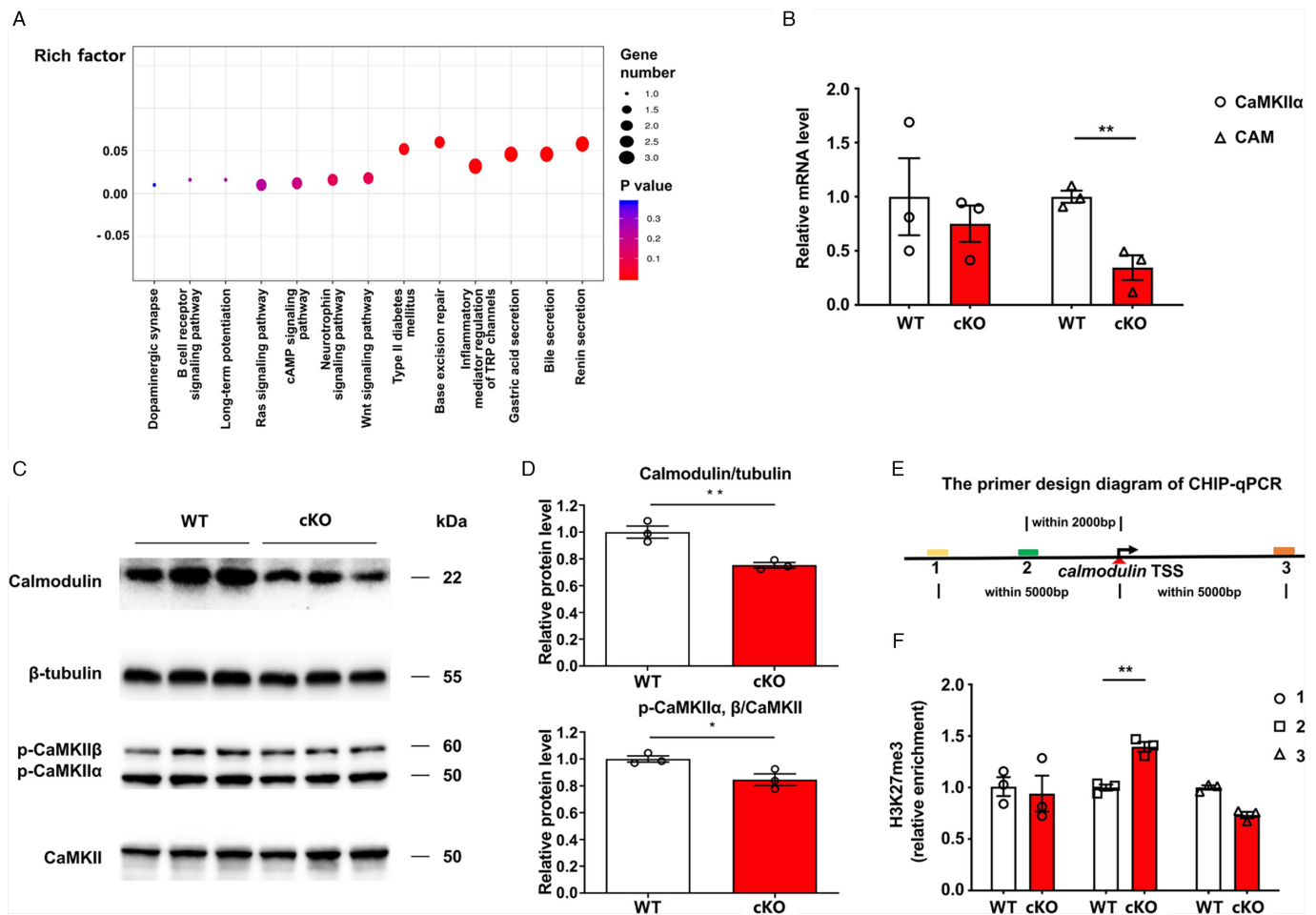


Figure 2 Loss of *UTX* downregulates calmodulin protein expression in the hippocampus by affecting the transcription of the calmodulin gene. (A) Top enriched pathways of differentially expressed genes in the hippocampus of *UTX* cKO mice. Rich factor is the ratio of the number of DEGs (Table S4) annotated in these pathways to the number of all genes annotated in these pathways. (B) The relative mRNA expression of the *CaMKIIα* and calmodulin (*CAM*) genes in the hippocampus of cKO mice normalised to that in the hippocampus of WT mice ($n=5$ from each group; $**p<0.01$, two-way ANOVA). (C, D) Western blotting showed the downregulation of calmodulin and phosphorylated *CaMKIIα* in the hippocampus of cKO mice at the protein level. The statistical quantification is shown in (D) ($n=3$ from each group; $*p<0.05$, $**p<0.01$, Student's *t*-test). (E) Amplicons (1–3) for real-time PCR are illustrated for calmodulin, a gene directly targeted by *UTX*. The black arrow represents the transcription start site for this gene. (F) Chip-qPCR showed that the enrichment of H3K27me3 on the promoter (amplicon 2) of the *UTX*-targeting gene calmodulin was significantly enhanced by the deletion of *UTX*. The enrichment of H3K27me3 upstream (amplicon 1) and downstream (amplicon 3) of the TSS for the target gene showed no change. Real-time PCR was performed on the input and immunoprecipitated genomic fragments. The data are presented as the percentage of input ($n=3$ for each group; $**p<0.01$, two-way ANOVA). All data are presented as the mean (SEM). ANOVA, analysis of variance; cAMP, cyclic adenosine monophosphate; ChIP, chromatin immunoprecipitation; cKO, conditional knockout; qPCR, quantitative PCR; SEM, standard error of the mean; TSS, transcription start site; TRP, transient receptor potential; WT, wild type.

cKO mice (figure 2A; online supplemental table 4). Using quantitative real-time PCR and western blotting, we confirmed the downregulation of calmodulin transcripts and protein expression in cKO mice (figure 2B–D). Calmodulin mediates important physiological processes, including remote memory.¹⁴ After binding with calcium ions, calmodulin phosphorylates *CaMKII* subunits and continuously activates *CaMKII*. *CaMKII* plays a key role in LTP formation and memory processes. Thus, we examined the phosphorylation level of *CaMKII* by immunoblotting. Indeed, loss of *UTX* in the brain conspicuously decreased phosphorylated *CaMKII* without changing transcription or

protein expression of *CaMKII* (figure 2B–D). Therefore, downregulation of calmodulin-*CaMKII* pathway activity might be the key molecular mechanism of impaired LTP and memory in *UTX*-deficient mice.

UTX regulates *Calmodulin* gene transcription through H3K27me3 demethylation

Previous studies have suggested that H3K27me3, predominantly located downstream of the transcription start site (TSS), may participate in active transcription.¹⁵ As an H3K27me3 demethylase, *UTX* binds to target genes at the TSS27 loci. To investigate how *UTX* regulates calmodulin gene expression, ChIP-qPCR assay was performed.

We quantitatively analysed the abundance of immunoprecipitated DNA fragments at the loci of TSS (amplicon 2), upstream (amplicon 1) and downstream (amplicon 3) of TSS (figure 2E) and found that the loss of *UTX* significantly increased the enrichment of H3K27me3 at the TSS of calmodulin (figure 2F). Thus, these data suggest that *UTX* specifically binds to the TSS of calmodulin and enhances calmodulin gene transcription by demethylating H3K27me3.

Desipramine rescues CaMKII activity, LTP and memory impairments

Considering the reduced CaMKII activity in *UTX*-deficient mice, we tested whether desipramine administration could ameliorate the LTP and memory deficits in *UTX* cKO mice. We first identified enhanced CaMKII activity following desipramine treatment in *UTX* cKO mice (figure 3B–D). Activated CaMKII can condense at the synapse through liquid-liquid phase separation.¹⁶

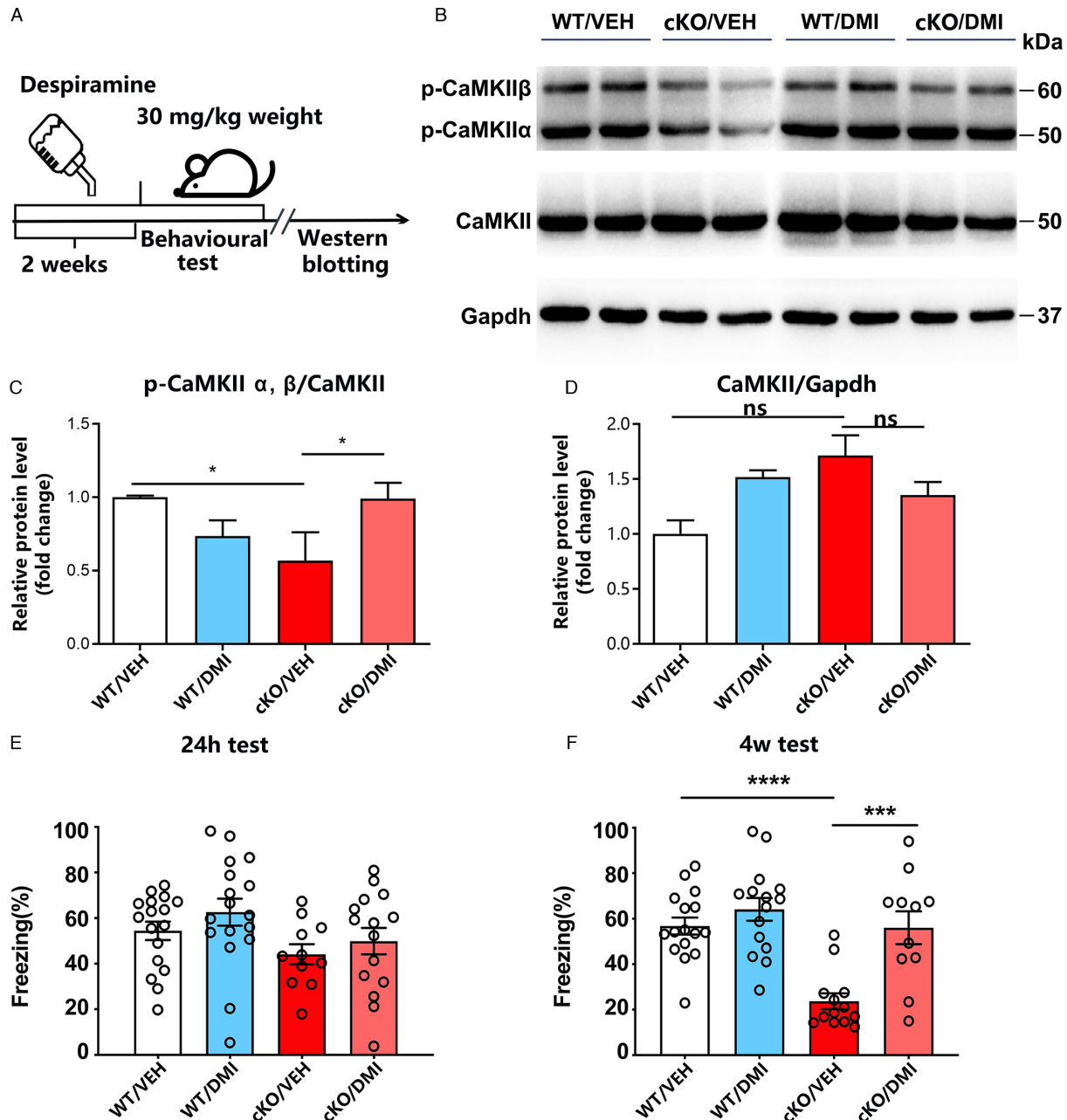


Figure 3 Desipramine rescues deficits in remote contextual fear conditioning in *UTX* cKO mice by reversing the decreased activity of CaMKII. (A) Desipramine treatment before the sample collection and the behavioural test. (B–D) Western blotting showed that desipramine reversed the decreased activity of CaMKII (n=2 for each group; *p<0.05, two-way ANOVA). (E, F) Results of contextual fear conditioning test at 24 hours and 4 weeks after training (24 hours: WT/VEH, n=17; WT/DMI, n=17; cKO/VEH, n=11; cKO/DMI, n=15; 4 weeks: WT/VEH, n=16; WT/DMI, n=15; cKO/VEH, n=13; cKO/DMI, n=11; ****p<0.001, ****p<0.0001, one-way ANOVA). All data are presented as the mean (SEM). ANOVA, analysis of variance; cKO, conditional knockout; DMI, desipramine; ns, non-significant; SEM, standard error of the mean; VEH, vehicle; WT, wild type.

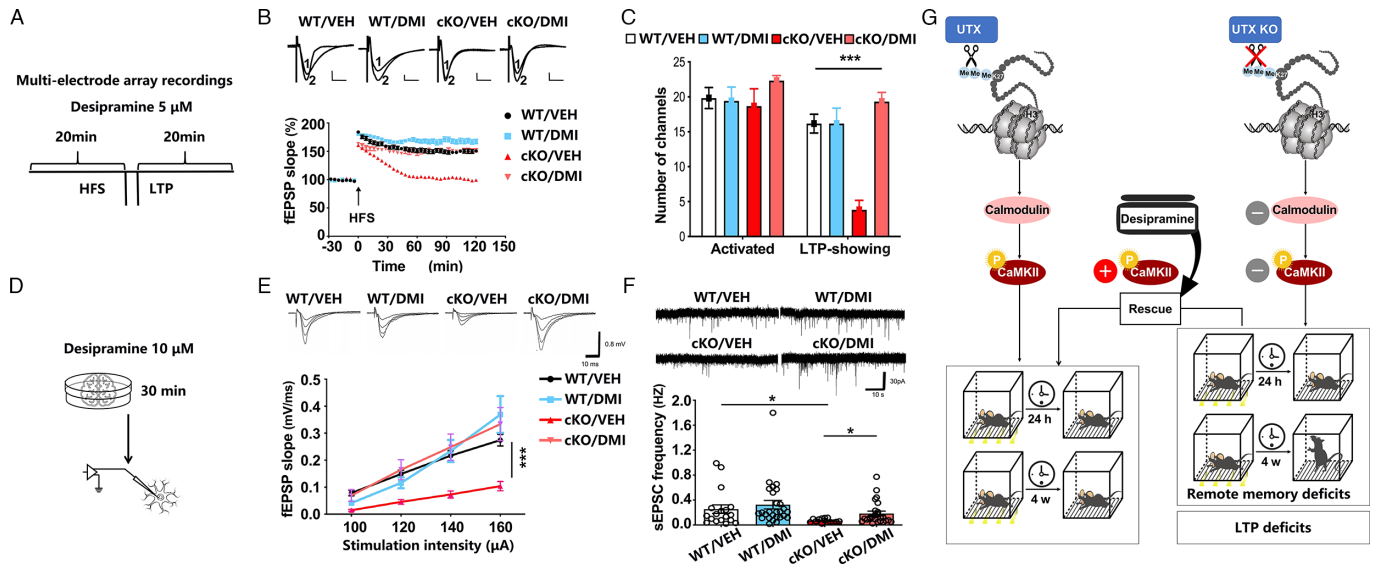


Figure 4 Desipramine rescues deficits in LTP and basal synaptic transmission in *UTX* cKO mice. (A) Desipramine treatment for the electrophysiological recording. (B) The slopes of fEPSPs before and after high-frequency stimulation were recorded from hippocampal slices. Desipramine did not affect LTP induction or maintenance in WT mice, and the deficiencies in LTP in *UTX* cKO mice were rescued by desipramine treatment ($n=6-7$ slices/ $5-7$ mice). (C) The number of activated and LTP-showing channels, assessed by two-way ANOVA ($n=6-7$ slices/ $5-7$ mice). (D) Desipramine treatment for the patch-clamp experiments. (E) The plot of I-O curves showing the relationship between the fEPSP slope and stimulation intensity at Schaffer collateral-CA1 synapses in hippocampal slices. There was a significant increase in fEPSP slope in cKO animals treated with desipramine compared with those treated with vehicle. The representative traces are shown at the top of the image (WT/VEH, $n=19$ slices from 6 mice; WT/DMI, $n=29$ slices from 9 mice; cKO/VEH, $n=15$ slices from 5 mice; cKO/DMI, $n=25$ slices from 10 mice; $***p<0.001$, two-way ANOVA). (F) Quantitative analysis of sEPSC frequency. The representative sEPSC traces recorded from WT and cKO mice are shown at the top of the image (WT/VEH, $n=18$ slices from seven mice; WT/DMI, $n=27$ slices from 9 mice; cKO/VEH, $n=14$ slices from five mice; cKO/DMI, $n=25$ slices from 10 mice; $*p<0.05$, Student's *t*-test). All data are presented as the mean (SEM). (G) A schematic diagram describing the mechanisms underlying *UTX* deletion-induced cognitive impairments. ANOVA, analysis of variance; cKO, conditional knockout; DMI, desipramine; fEPSPs, field excitatory postsynaptic potentials; HFS, high-frequency stimulation; LTP, long-term potentiation; SEM, standard error of the mean; sEPSC, spontaneous excitatory postsynaptic current; VEH, vehicle; WT, wild type.

Activated CaMKII and NMDAR2B facilitate the coalescence of AMPARs and the synaptic adhesion molecule neuroligin into a phase-in-phase assembly.¹⁷ Thus, we also investigated the profile of receptors downstream of CaMKII. The ratios of pNMDAR2B/NMDAR2B and pAMPA1/AMPA1 were decreased in *UTX* cKO mice, while the total expression of these receptors remains unchanged (online supplemental figure 3). We next assessed learning and memory performance in *UTX* cKO mice after desipramine administration. Desipramine treatment increased the freezing percentage of cKO mice in the 4-week contextual fear conditioning test to levels comparable to those of the vehicle-treated WT group (figure 3E,F).

Furthermore, we examined the effect of desipramine on abnormal hippocampal LTP and synaptic transmission in *UTX* cKO mice. The results showed that desipramine treatment significantly reversed LTP impairments (figure 4B,C), deficiencies in the input/output curves (figure 4E) and abnormalities in spontaneous EPSC frequency (figure 4F). We also recorded LTP after intra-hippocampal injection of AAV-CaMKII-CRE virus in *UTX* f/y mice. The results demonstrate that LTP is impaired in cKO mice, which was rescued by desipramine

administration (online supplemental figure 4). Furthermore, desipramine treatment rescued the deficits of neuronal morphology in *UTX* cKO mice, including decreases in dendritic arborisation complexity, total dendritic length and the number of branches (online supplemental figure 1). Taken together, these findings indicate that desipramine treatment rescues deficits in the calmodulin-CaMKII signalling pathway, reverses the abnormal synaptic transmission and plasticity, and thereby rescues learning and memory deficits in *UTX* cKO mice.

DISCUSSION

Main findings

Previous studies have shown that histone methylation is involved in the regulation of learning and memory signalling pathways.¹⁸ Histone demethylase encoding gene *UTX* is a key pathogenic risk gene of KS,¹⁹ highlighting its important role in the nervous system, especially in cognitive function. Here, we found that *UTX* cKO mice displayed remote fear memory deficits, indicating the critical role of *UTX* in the regulation of learning and memory.

UTX is a pathogenic risk gene for KS,¹⁹ a condition characterised by congenital developmental abnormalities and mental disorders. *UTX* specifically removes methyl groups from histone 3 dimethylated or trimethylated at lysine 27 (H3K27me_{2/3} methyl group), promoting gene transcription. Given the role of histone 3 methylation and demethylation in modulating the expression of memory-related genes,²⁰ we speculate that impaired *UTX* expression may result in abnormal histone 3 methylation and induce memory deficit. To investigate the role of *UTX* in learning and memory, we generated a *UTX* cKO mouse model. Our data support the hypothesis that *UTX* regulates methylation-induced memory deficit and indicate that *UTX* deletion downregulates calmodulin transcription by disrupting H3K27me₃ demethylation.

Interestingly, *UTX* cKO mice presented a significant memory impairment at 4 weeks after aversive stimulus (ie, the electric shocks during fear conditioning training), while the contextual memory tested at 24 hours after training remained unaffected. This may be attributed to the dynamic nature of memory storage, where long-term memories do not form immediately after learning but develop with time,^{21 22} and de novo gene expression governed by the epigenome necessary for memory stabilisation requires at least 24 hours.²³ Additionally, the experience of fear can induce persistent activity-specific transcriptional alterations that last for weeks.²⁴

Long-term synaptic plasticity, a synaptic network in which the number or type of synaptic connections changes in response to learning, is an important mechanism underlying the formation and storage of memory.²⁵ This process, which involves the expression of plasticity-related proteins required to construct and sustain long-lasting synaptic alterations, typically takes time ranging from hours to days.²⁶ In our study, *UTX* cKO mice presented a cognitive dysfunction only at 4 weeks but not 24 hours after training, possibly due to the disrupted synaptic connection and neuron morphology.

Hippocampal activity-dependent LTP is proposed as a major cellular mechanism of learning and memory. Indeed, it has long been suggested that LTP impairment results in memory deficit via calmodulin-CaMKII signalling pathway.²⁷ Specifically, CaMKII phosphorylation which occurs at Thr286 is activated by calcium-bound calmodulin through a direct binding mechanism that is critical for LTP induction and the memory process.²⁸ In the current study, we observed that LTP was impaired in *UTX* cKO mice. Furthermore, we found that the expression level of calmodulin was downregulated through disruption of H3K27me₃ binding with the promoter region of calmodulin, which directly led to decreased CaMKII phosphorylation at Thr286 site in *UTX* cKO mouse, suggesting that *UTX* plays a critical role in maintaining LTP via calmodulin-CaMKII pathway.

Phosphorylation of glutamate receptors, including AMPA and NMDA receptors, is considered to underlie the transmission regulation in LTP and is mediated by CaMKII.²⁹ Here, we examined the phosphorylation of

AMPA and NMDA receptors, and found that both were decreased in *UTX* cKO mice. Interestingly, our result showed that the sEPSC frequency was also decreased in *UTX* cKO mice, contrary to previous studies reporting that decreased phosphorylation of AMPA and NMDA receptors led to reduced sEPSC amplitude instead of frequency. This highlights the needs for further studies to understand the complex role of *UTX* in synaptic transmission. Overall, *UTX* deficit in mouse results in decreased expression of calmodulin, leading to impaired CaMKII phosphorylation, therefore decreasing the phosphorylation of AMPA and NMDA receptors, and ultimately causing LTP abnormality and remote memory deficits. Importantly, all these effects could be rescued with desipramine treatment, further supporting our finding that *UTX* deficiency results in LTP impairment via modulating the calmodulin-CaMKII pathway.

In summary, KS is a rare developmental disorder and its pathogenesis remains elusive. In this study, we explored how the deficiency of *UTX*, a primary pathogenic risk gene of KS, leads to plasticity and memory deficits. Through RNA-seq analysis, we examined several critical signalling pathways in *UTX* cKO mice, including the calmodulin-CaMKII pathway. The rescue effect of desipramine treatment on synaptic and cognitive deficits observed in this study may provide a potential therapeutic target for KS. In addition to the calmodulin-CaMKII pathway, our study identified several other pathways known to be involved in memory regulation in *UTX* cKO mice, including the dopaminergic pathway, Ras signalling pathway and cAMP signalling pathway.³⁰ Whether these pathways are involved in the synaptic plasticity and memory deficits observed in *UTX* cKO mice need to be further studied.

Limitations

This study focused on exploring how the deficiency of *UTX* results in memory deficits in a mouse model. Therefore, the translation of *UTX* mechanism in cognition into clinical practice requires further research in the future.

Implications

We showed that the negative effects of *UTX* deletion on synaptic plasticity and memory could be reversed by an Food and Drug Administration (FDA)-approved drug, desipramine. The development of specialised drugs for rare diseases is a costly and undermotivated endeavour, whereas indication expansion of currently available drugs can effectively address this issue. Desipramine has undergone rigorous approval by the FDA and has been extensively validated through numerous clinical trials, with its pathotoxicological mechanisms clearly elucidated. For individuals with KS, rapid access to desipramine is available, eliminating the need for extended mechanistic trials traditionally required for the approval of novel therapeutic drugs. Although the results of this study should be considered preliminary and require further clinical validation, the therapeutic effect of desipramine on synaptic and cognitive deficits observed in this study

supports further exploration of desipramine as a promising potential target for KS.

Author affiliations

¹Bio-X Institutes, Key Laboratory for the Genetics of Development and Neuropsychiatric Disorders (Ministry of Education), Brain Health and Brain Technology Center at Global Institute of Future Technology, Institute of Psychology and Behavioral Science, Shanghai Jiao Tong University, Shanghai, China

²Department of Anatomy and Physiology, Shanghai Jiao Tong University School of Medicine, Shanghai, China

³Institute of Mental Health and Drug Discovery, Oujian Laboratory, Wenzhou, Zhejiang, China

⁴Shanghai Institutes for Biological Sciences, Chinese Academy of Sciences, Shanghai, China

⁵Shinshu University School of Medicine, Nagano, Japan

⁶Western University of Health Sciences, Pomona, California, USA

⁷WLA Laboratories, World Laureates Association, Shanghai, China

Acknowledgements We thank Dr Emilie Marcus (Executive Strategy Officer at David Geffen School of Medicine at UCLA) for her valuable comments on preparing this manuscript.

Contributors LC, YL, ML, XZ, XY and SW contributed to performing the experiments. ZL, YK, YZ and ET contributed to analysing the data. MZ ameliorated statistical methods. CDC and LX generated Utx f/f mice. LC, YL, ML, ZL, MZ and WL contributed to writing the manuscript. TS, KT and TX contributed to the design of the experiment. WL designed the experiments and supervised the project. WL is responsible for the overall content as the guarantor. WL accepts full responsibility for the finished work and the conduct of the study, had access to the data, and controlled the decision to publish.

Funding This work was supported by STI2030-Major Projects (2022ZD0204900), the National Natural Science Foundation of China (NSFC) (91632103, 31900732, 31771157); the Program of Shanghai Subject Chief Scientist (17XD1401700), National Key Research and Development Program of China (2018YFE0126700), the Shanghai Education Commission Research and Innovation Program (2019-01-07-00-02-E00037), Natural Science Foundation of Chongqing cstc2021jcyj-msxmX1176, the '111' Program of Higher Education Discipline Innovation, 'Eastern Scholar' (Shanghai Municipal Education Commission), Shanghai Municipal Commission of Science and Technology Program (21dz2210100), China Postdoctoral Science Foundation (202N1702133, 2021M702137). The National Science Fund for Distinguished Young Scholars (31900732).

Competing interests None declared.

Patient consent for publication Not applicable.

Ethics approval Animal experiments were conducted in accordance with 'NIH Guidelines for the Care and Use of Laboratory Animals'. The Institutional Animal Care and Use Committee (IACUC) of Shanghai Jiao Tong University approved this study. The approved animal protocol number is A2016021 and A2020038-2.

Provenance and peer review Not commissioned; externally peer reviewed.

Data availability statement All data relevant to the study are included in the article or uploaded as supplementary information.

Supplemental material This content has been supplied by the author(s). It has not been vetted by BMJ Publishing Group Limited (BMJ) and may not have been peer-reviewed. Any opinions or recommendations discussed are solely those of the author(s) and are not endorsed by BMJ. BMJ disclaims all liability and responsibility arising from any reliance placed on the content. Where the content includes any translated material, BMJ does not warrant the accuracy and reliability of the translations (including but not limited to local regulations, clinical guidelines, terminology, drug names and drug dosages), and is not responsible for any error and/or omissions arising from translation and adaptation or otherwise.

Open access This is an open access article distributed in accordance with the Creative Commons Attribution Non Commercial (CC BY-NC 4.0) license, which permits others to distribute, remix, adapt, build upon this work non-commercially, and license their derivative works on different terms, provided the original work is properly cited, appropriate credit is given, any changes made indicated, and the use is non-commercial. See: <http://creativecommons.org/licenses/by-nc/4.0/>.

ORCID iDs

Yuting Li <http://orcid.org/0000-0002-4668-6373>

Shuai Wang <http://orcid.org/0000-0002-9252-7496>

REFERENCES

- Courstens W, Rassart A, Stene JJ, *et al*. Further evidence for autosomal dominant inheritance and ectodermal abnormalities in Kabuki syndrome. *Am J Med Genet* 2000;93:244–9.
- Carromeu C, Vessoni A, Mendes A. Differentiation of human pluripotent stem cells into cortical neurons. In: *Working with stem cells*. Springer, 2016.
- Wang YR, Xu NX, Wang J, *et al*. Kabuki syndrome: review of the clinical features, diagnosis and epigenetic mechanisms. *World J Pediatr* 2019;15:528–35.
- Shan Y, Zhang Y, Zhao Y, *et al*. JMJD3 and UTX determine fidelity and lineage specification of human neural progenitor cells. *Nat Commun* 2020;11:382.
- Paděrová J, Holubová A, Simandlová M, *et al*. Molecular genetic analysis in 14 Czech Kabuki syndrome patients is confirming the utility of phenotypic scoring. *Clin Genet* 2016;90:230–7.
- Wang Y, Khandelwal N, Liu S, *et al*. KDM6B cooperates with tau and regulates synaptic plasticity and cognition via inducing VGLUT1/2. *Mol Psychiatry* 2022;27:5213–26.
- Lee S, Lee JW, Lee SK. UTX, a histone H3-lysine 27 demethylase, acts as a critical switch to activate the cardiac developmental program. *Dev Cell* 2012;22:25–37.
- Tang Q-Y, Zhang S-F, Dai S-K, *et al*. UTX regulates human neural differentiation and dendritic morphology by resolving bivalent promoters. *Stem Cell Reports* 2020;15:439–53.
- Celano E, Tiraboschi E, Consogno E, *et al*. Selective regulation of presynaptic calcium/calmodulin-dependent protein kinase II by psychotropic drugs. *Biol Psychiatry* 2003;53:442–9.
- Kang SJ, Liu M-G, Chen T, *et al*. Plasticity of metabotropic glutamate receptor-dependent long-term depression in the anterior cingulate cortex after amputation. *J Neurosci* 2012;32:11318–29.
- Holtmaat A, Svoboda K. Experience-dependent structural synaptic plasticity in the mammalian brain. *Nat Rev Neurosci* 2009;10:647–58.
- Grutzendler J, Tsai J, Gan WB. Rapid labeling of neuronal populations by ballistic delivery of fluorescent dyes. *Methods* 2003;30:79–85.
- Maren S, Phan KL, Liberzon I. The contextual brain: implications for fear conditioning, extinction and psychopathology. *Nat Rev Neurosci* 2013;14:417–28.
- Cohen SM, Suutari B, He X, *et al*. Calmodulin shuttling mediates cytonuclear signaling to trigger experience-dependent transcription and memory. *Nat Commun* 2018;9:2451.
- Rice JC, Briggs SD, Ueberheide B, *et al*. Histone methyltransferases direct different degrees of methylation to define distinct chromatin domains. *Mol Cell* 2003;12:1591–8.
- Hayashi Y. Molecular mechanism of hippocampal long-term potentiation - towards multiscale understanding of learning and memory. *Neurosci Res* 2022;175:3–15.
- Hosokawa T, Liu P-W, Cai Q, *et al*. CaMKII activation persistently segregates postsynaptic proteins via liquid phase separation. *Nat Neurosci* 2021;24:777–85.
- Day JJ, Sweatt JD. Epigenetic mechanisms in cognition. *Neuron* 2011;70:813–29.
- Makrythanasis P, van Bon BW, Steehouwer M, *et al*. MLL2 mutation detection in 86 patients with kabuki syndrome: a genotype-phenotype study. *Clin Genet* 2013;84:539–45.
- Colvis CM, Pollock JD, Goodman RH, *et al*. Epigenetic mechanisms and gene networks in the nervous system. *J Neurosci* 2005;25:10379–89.
- Bailey CH, Bartsch D, Kandel ER. Toward a molecular definition of long-term memory storage. *Proc Natl Acad Sci U S A* 1996;93:13445–52.
- Corbett D, Murphy K. Regulation of transcription factors during memory consolidation. Sfn - Society for Neuroscience; 2014.
- Alberini CM, Johnson SA, Ye X. *Memory reconsolidation: lingering consolidation and the dynamic memory trace*. Academic Press, 2013.
- Chen MB, Jiang X, Quake SR, *et al*. Persistent transcriptional programmes are associated with remote memory. *Nature New Biol* 2020;587:437–42.
- Nicoll RA, Schulman H. Synaptic memory and CaMKII. *Physiol Rev* 2023;103:2877–925.
- Dieterich DC, Hodas JLL, Gouzer G, *et al*. In situ visualization and dynamics of newly synthesized proteins in rat hippocampal neurons. *Nat Neurosci* 2010;13:897–905.
- Zalcman G, Federman N, Romano A. CaMKII isoforms in learning and memory: localization and function. *Front Mol Neurosci* 2018;11:445.

- 28 Giese KP, Fedorov NB, Filipkowski RK, *et al.* Autophosphorylation at Thr-286 of the alpha calcium-calmodulin kinase II in LTP and learning. *Science* 1998;870–3.
- 29 Wang JQ, Guo M-L, Jin D-Z, *et al.* Roles of subunit phosphorylation in regulating glutamate receptor function. *Eur J Pharmacol* 2014;728:183–7.
- 30 Noyes NC, Walkinshaw E, Davis RL. Ras acts as a molecular switch between two forms of consolidated memory in *Drosophila*. *Proc Natl Acad Sci U S A* 2020;117:2133–9.



Lei Chen obtained her PhD degree from Bio-X Institute of Shanghai Jiao Tong University, China in 2018, and has been a postdoctoral researcher there since then. Her current research activities and interests focus on the learning and memory mechanisms in various mouse models, including the role of epigenetics in cognitive functions (especially on the molecular mechanism of UTX in learning and memory), the pathogenic mechanisms and molecular pathways of rare neuropsychiatric disorders. She also participates in studies on neural circuit and iPSC. She led a research project funded by the National Natural Science Foundation of China (Youth Foundation) from 2020 to 2022, further developing her expertise in neuroscience and gaining valuable insights into the complex interplay between epigenetics, molecular pathways, and cognitive functions.